Direct determination of the wave field of an x-ray nanobeam

Hidekazu Mimura,[1,*] Hirokatsu Yumoto,[1] Satoshi Matsuyama,[1] Soichiro Handa,[1] Takashi Kimura,[1] Yasuhisa Sano,[1] Makina Yabashi,[2] Yoshinori Nishino,[3] Kenji Tamasaku,[3] Tetsuya Ishikawa,[3] and Kazuto Yamauchi[1]

[1]*Department of Precision Science and Technology, Graduate School of Engineering, Osaka University, 2-1 Yamada-oka, Suita, Osaka, 565-0871, Japan*

[2]*Japan Synchrotron Radiation Research Institute (JASRI)/SPring-8, 1-1-1 Kouto, Sayo-cho, Sayo-gun Hyogo, 679-5148, Japan*

[3]*RIKEN/SPring-8, 1-1-1 Kouto, Sayo-cho, Sayo-gun, Hyogo, 679-5148, Japan*

(Received 21 May 2007; published 31 January 2008)

We present a remarkably accurate method for determining the wave field of an x-ray nanobeam. The intensity profile of a beam was directly measured over a range of three orders of magnitude while its phase distribution was successfully recovered using an iterative algorithm. The evolution of the wave field along the beam propagation direction was precisely simulated, and there was good agreement with the experimental results.

DOI: 10.1103/PhysRevA.77.015812 PACS number(s): 42.15.Eq, 41.50.+h, 07.85.Fv

The minimum spot size of a focused photon beam is determined by the wavelength employed. This principle has stimulated x-ray physicists to produce extremely small focused spots of x rays. Focused beams require ideal wave fronts both for focusing to small spot sizes and for applications such as holography [1] and diffraction microscopy [2,3].

Major obstacles in focusing x-ray beams to ultimate sizes below 10 nm are the requirements for unprecedented levels of both accuracy of alignment and quality of optics. An effective way to overcome these obstacles is to analyze and compensate wave-front errors during focusing experiments. In the wavelength range from visible light to extreme ultraviolet radiation, the exact wave-front error in an imaging optical system can be measured by point diffraction interferometry [4] since the spherical wave produced by a pinhole acts as a sufficiently ideal reference light. In the hard x-ray range, however, it is almost impossible to generate a reference beam that can interfere with a test beam to produce measurable interference fringes. An alternative method for measuring the wave front of x rays is the phase retrieval method proposed by J. R. Fienup [5] as an optical metrology tool. This method determines the wave-front error by measuring only x-ray intensity profiles near the focal plane; it, however, requires exact intensity profiles, including the structures of satellite peaks [6].

Hard x-ray beams having diameters smaller than 50 nm have been achieved using several optical systems [7–10]. Precise measurement of the beam's profile near the focus is becoming quite difficult as spot sizes decrease. Thus, a method for accurately analyzing the x-ray nanobeams is strongly desired. For this reason, a method was proposed for reconstructing the wave field from the far-field intensity distribution based on phase retrieval calculations [11], although this is still an indirect approach for evaluating beam profiles near the focus.

A knife-edge scan method has been conventionally employed for probing the intensity distribution; this method involves recovering the original profile by differentiating the transmitted intensity with respect to the edge position. However, a fundamental limitation of this method is that the depth of the focus, which can be as small as a few microns, can be shorter than the x-ray attenuation length of the edge material. A method without differentiation process has been used to measure intensity profiles whose size was ~20 nm. In these methods, fluorescent x rays from a minute pattern [9] and the x rays diffracted from the knife edge [10] are employed as signals. However, the signal-to-noise ratios that have been achieved using this method are insufficient to reproduce the satellite peak structure.

In this Brief Report, we present the nanometer-resolution direct intensity measurement and the determination of complex amplitude of an x-ray nanobeam produced by an ultraprecisely figured mirror.

Figure 1 shows a schematic diagram of the method employed in this study. When an object is inserted in the path of a propagating light beam, the wave field of the light behind the object can be expressed as the sum of the geometrical

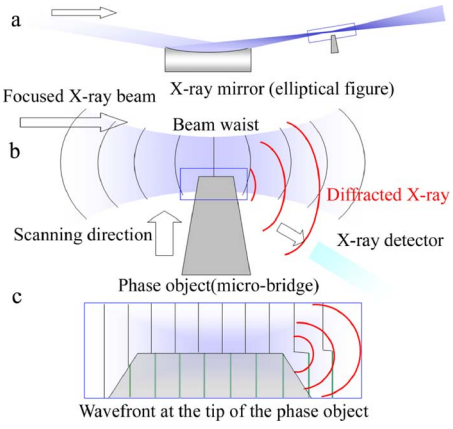

FIG. 1. (Color online) Schematic diagram of x-ray intensity distribution sensing system using a microphase object (microbridge structure). (a) Hard x rays are focused by reflective optics. (b) Enlarged diagram of wave front in the vicinity of the beamwaist. (c) Wave front above and inside the microphase object.

*mimura@prec.eng.osaka-u.ac.jp

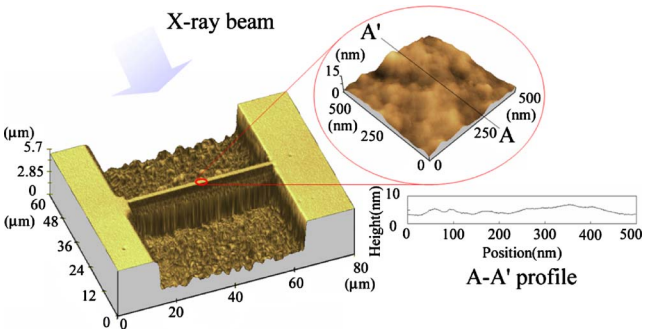

FIG. 2. (Color online) Microbridge structure used for measuring the intensity distributions of a hard x-ray line-focused beam. These images were obtained using a nanosearch microscope (Shimadzu Co.) that incorporates both a scanning confocal laser microscope and an atomic force microscope.

optics field and the diffraction field. In the case under consideration, the latter is a cylindrical wave diffracted from the edge of the object [see Figs. 1(b) and 1(c)]. This concept is generally referred to as Sommerfeld's solution in rigorous diffraction theory [12]. The intensity of the cylindrical wave is assumed to be proportional to the intensity of the propagating light that illuminates the edge. The object inserted into the beam (see Fig. 1) had the microbridge structure shown in Fig. 2.

A platinum layer having a thickness of approximately 2 μm was deposited on a Si(001) wafer surface. We used an electron beam deposition system (Alvuc Co). The microbridge structure that was approximately 2 μm wide in the beam direction and 50 μm long was fabricated using a focused ion beam fabrication system. The focused Ga ion beam had a diameter of approximately 20 nm. Care was taken not to generate any roughness on the surface of the bridge during machining. In addition, the ion beam was never scanned on the surface of the microbridge. The surface roughness of the bridge was directly measured and it was confirmed to be of nanometer-order flatness having peak-to-valley height of 3.02 nm. The transmissivity and the phase shift of the x-ray beam passing through the 2-μm-thick platinum block were 50% and π radians, respectively. The cylindrical wave is efficiently generated at the boundary in this case. The microbridge was designed to have a trapezoidal profile so that x rays which propagate through the platinum are deflected upwards; this ensures that only diffracted x rays are detected in the lower region behind the microbridge where the x-ray detector is located. The spatial resolution that can be achieved when measuring the intensity profile depends on the flatness of the microbridge surface. The resolution of our system is expected to be better than 3 nm based on the atomic force microscope image shown in Fig. 2.

A precisely shaped x-ray mirror with an elliptical profile was used to generate the x-ray nanobeam. It should be noted that x-ray focusing mirrors are leading components from the viewpoint of beam size and focusing efficiency [7] and that they are promising focusing optics for x-ray free-electron lasers due to the high radiation hardness that can be achieved using them. The mirror surface was fabricated by computer-controlled figuring using accurately measured surface profile data [13–15]. The main machining method was elastic emission machining with a removal depth controllability of 0.1 nm and a spatial resolution of 0.3 mm in figuring. Metrology consisting of microstitching interferometry and relative angle determinable stitching interferometry was specially developed for measuring the surface profiles of the x-ray focusing mirror.

The root-mean-square surface roughness was smaller than 0.2 nm along the mirror length of 96 mm. The average incident angle was 3.9 mrad and the focal length was 128 mm. The theoretical focal beam size (defined as the full width at half maximum of the intensity profile) was 30 nm.

An experiment to analyze the line-focused beam using the microbridge structure was performed at the 1 km beamline of SPring-8. A monochromatic x-ray beam with a photon energy of 15 keV was selected using a Si(111) monochromator and guided to an experimental station located 1 km from the monochromator, where a coherent x-ray beam with a large area was available [16]. A piezoactuated translation stage enabled microbridge scanning in 1 nm increments. Alignment for optimizing the focusing condition was performed by monitoring the intensity profile. The orientation of the microbridge relative to the line-focused beam was finely adjusted while viewing a magnified shadow image of the projected x-ray image obtained using a 700-nm-resolution x-ray imaging system. An avalanche photodiode detector, which had good linearity even down to extremely low photon levels, was used to detect the diffracted x rays by putting it in the lower region of the magnified x-ray image, as shown in Fig. 1.

Figure 3(a) shows a linear graph and Fig. 3(b) shows a semilogarithmic graph of the intensity distribution profile measured in the focal plane. The focal width was found to be 32 nm and this value is in good agreement with the theoretical value of 30 nm. The logarithmic plot shows that the third-order satellite peak structures are distinguishable. Approximately 50 000 photons were counted at the top of the main peak; in contrast, only ~50 photons were detected in the third-order position, demonstrating that this method can achieve an excellent signal-to-noise ratio. When an avalanche photodiode detector was positioned in the upper region of the magnified x-ray image, the intensity profile could not be measured due to the very high noise as a result of the x rays reflected and scattered from the microbridge.

A phase retrieval calculation was coded for determining the phase error distributions on a mirror using only the intensity profile of a focused x-ray beam. Figure 3(d) shows the figure error profile calculated using phase retrieval methods using only this intensity profile, together with the one measured using an interferometric surface profiler after mirror fabrication. The two profiles are in good agreement within a 1 nm level corresponding to a wave-front error of 0.15 wave.

The wave-field distribution along the beam propagation direction near the focus was numerically simulated [Fig. 4(b)] by calculating the Fresnel-Kirchhoff integral, using the recovered surface profile shown in Fig. 3(d) [17]. For comparison, the wave-field distribution shown in Fig. 4(a) is the calculated result for the ideal surface profile shown in Fig. 3(c). The beamwaist structure of the former was slightly dis-

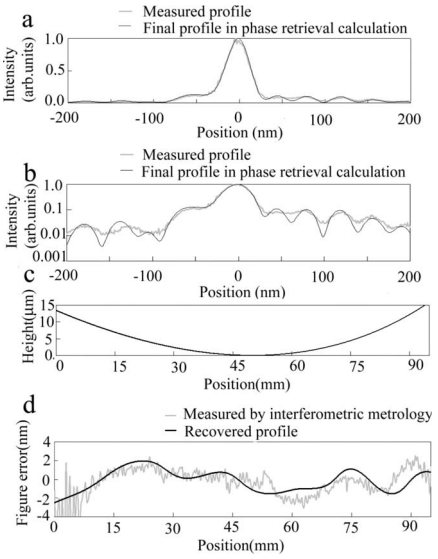

FIG. 3. Results of measuring intensity profiles in the focal plane and phase retrieval calculations. (a) Intensity profiles in the focal plane. The gray line is the profile measured by scanning the microbridge, while the black line was obtained using phase retrieval calculations for determining the mirror surface profile. The plot interval is 1 nm. (b) Single logarithmic plot of graph in (a). (c) Ideal profile of x-ray mirror. (d) Comparison of measured and reconstructed figure error profiles.

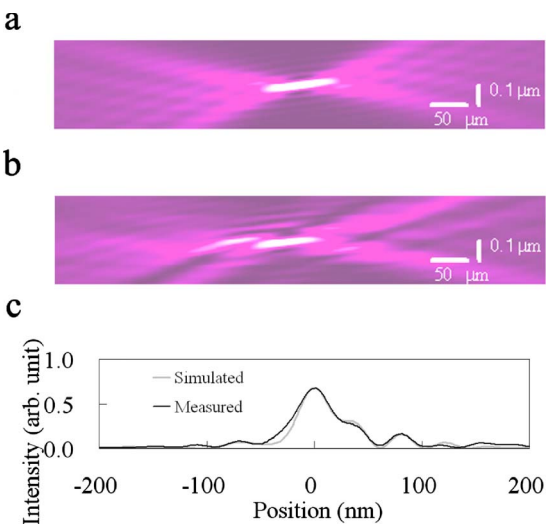

FIG. 4. (Color online) Simulation results of intensity distributions of a line-focused hard x-ray beam near the focus. (a) Ideal intensity distribution near the focus. (b) Intensity distribution near the focus, calculated using the recovered figure error profile of Fig. 3(d). (c) Intensity profile measured and simulated 50 μm upstream from the focal plane.

torted due to surface figure errors. To enable a more quantitative comparison, the transverse cross section of the simulated profile at 50 μm upstream from the focal plane was compared to that measured by scanning the microbridge [see Fig. 4(c)]. There is reasonable agreement between the two profiles, indicating that the complex amplitude around the focus was precisely reproduced.

Wave-front control of an x-ray beam entering a focusing device is an effective means of compensating the recovered phase error. For example, adaptive mirror optics having a figure controllability of 1 nm can be used to control the wave-front profile of a totally reflected x-ray beam to an accuracy below 0.1 wave for the grazing incidence condition. We consider that this compensation method will enable x-ray beams to be focused to spot sizes of the order of 1 nm, which is approaching the fundamental limit for the minimum size of a focused x-ray beam [18,19].

To date, methods of evaluating x-ray nanobeams have been preceded by the development of focusing optics. It is anticipated that the method presented in this paper that uses a microbridge structure will be widely applicable for evaluating all x-ray focusing devices. In particular, information concerning the complex phase and intensity near the focus is indispensable for x-ray free-electron lasers applications. This x-ray intensity measurement method combined with phase retrieval calculations promises to contribute to a breakthrough in the development of advanced x-ray focusing optics and various investigations of x-ray microscopy.

This research was supported by a Grant-in-Aid for Specially Promoted Research 18002009, 2006 and 21st Century COE Research, Center for Atomistic Fabrication Technology, 2006 from the Ministry of Education, Sports, Culture, Science and Technology, Japan. The use of BL29XU at SPring-8 was supported by RIKEN.

[1] S. Eisebitt, J. Lüning, W. F. Schlotter, M. Lörgen, O. Hellwig, W. Eberhardt, and J. Stöhr, Nature (London) **432**, 885 (2004).
[2] J. Miao, P. Charalambous, J. Kirz, and D. Sayre, Nature (London) **400**, 342 (1999).
[3] G. J. Williams, H. M. Quiney, B. B. Dhal, C. Q. Tran, K. A. Nugent, A. G. Peele, D. Paterson, and M. D. deJonge, Phys. Rev. Lett. **97**, 025506 (2006).
[4] R. N. Smart and W. H. Steel, Jpn. J. Appl. Phys. **14**, 351 (1975).
[5] J. R. Fienup, Appl. Opt. **21**, 2758 (1982).
[6] H. Yumoto, H. Mimura, S. Matsuyama, S. Handa, Y. Sano, M. Yabashi, Y. Nishino, K. Tamasaku, T. Ishikawa, and K. Yamauchi, Rev. Sci. Instrum. **77**, 063712 (2006).
[7] H. Mimura *et al.*, Appl. Phys. Lett. **90**, 051903 (2007).
[8] C. G. Schroer, M. Kuhlmann, T. F. Günzler, B. Lengeler, M. Richwin, B. Griesebock, D. Lützenkirchen-Hecht, R. Frahm, and E. Ziegler, Appl. Phys. Lett. **82**, 3360 (2003).
[9] H. C. Kang, J. Maser, G. B. Stephenson, C. Liu, R. Conley, A. T. Macrander, and S. Vogt, Phys. Rev. Lett. **96**, 127401 (2006).
[10] Y. Suzuki, A. Takeuchi, H. Takano, and H. Takenaka, Jpn. J. Appl. Phys., Part 1 **44**, 1994 (2005).

[11] H. M. Quiney, A. G. Peele, Z. Cai, D. Paterson, and K. A. Nugent, Nat. Phys. **2**, 101 (2006).
[12] M. Born and E. Wolf, *Principles of Optics*, 6th ed. (Cambridge University Press, Cambridge, England, 1997).
[13] K. Yamauchi, H. Mimura, K. Inagaki, and Y. Mori, Rev. Sci. Instrum. **73**, 4028 (2002).
[14] K. Yamauchi *et al.*, Rev. Sci. Instrum. **74**, 2894 (2003).
[15] H. Mimura *et al.*, Rev. Sci. Instrum. **76**, 045102 (2005).
[16] K. Tamasaku, Y. Tanaka, M. Yabashi, H. Yamazaki, N. Kawamura, M. Suzuki, and T. Ishikawa, Nucl. Instrum. Methods Phys. Res. A **467-468**, 686 (2001).
[17] K. Yamauchi *et al.*, Appl. Opt. **44**, 6927 (2005).
[18] C. Bergemann, H. Keymeulen, and J. F. van der Veen, Phys. Rev. Lett. **91**, 204801 (2003).
[19] C. G. Schroer and B. Lengeler, Phys. Rev. Lett. **94**, 054802 (2005).